




Transition from degeneracy to coalescence: Theorem and applicationsP. Wang , K. L. Zhang , and Z. Song ^{*}*School of Physics, Nankai University, Tianjin 300071, China*

(Received 28 July 2021; revised 18 November 2021; accepted 28 November 2021; published 7 December 2021)

An exceptional point (EP) is exclusive for non-Hermitian systems and distinct from that at a degeneracy point (DP), supporting intriguing dynamics which can be utilized to probe quantum phase transitions and prepare eigenstates in a Hermitian many-body system. In this paper, we investigate the transition from a DP for a Hermitian system to an EP driven by non-Hermitian terms. We present a theorem on the existence of a transition between a DP and EP for a general system. Specifically, one of twofold degenerate eigenstates of a Hermitian system becomes a coalescing state when a selected non-Hermitian term is added. The obtained EP is robust to the strength of non-Hermitian terms. We illustrate the theorem by an exactly solvable quasi-one-dimensional model, which allows for the existence of a transition between fully degenerate and exceptional spectra driven by non-Hermitian tunnelings in real and k spaces, respectively. We also study the EP dynamics for generating coalescing edge modes in Su-Schrieffer-Heeger-like models. This finding reveals the ubiquitous connection between DPs and EPs.

DOI: [10.1103/PhysRevB.104.245406](https://doi.org/10.1103/PhysRevB.104.245406)**I. INTRODUCTION**

Theoretical [1–3] and experimental studies [4–14] on non-Hermitian systems indicate that the interplay of lattice geometry and non-Hermitian elements, such as an imaginary on-site potentials [15,16] and asymmetry tunneling [17], can induce exotic quantum dynamics [18–22], which never happens in Hermitian systems. Intuitively, these phenomena are known to arise from the appearance of complex eigenenergies within a symmetry-broken region, leading to the explosion of the Dirac probability of the eigenstate. However, it follows from a peculiar feature of the non-Hermitian system, the exceptional point (EP) dynamics, without the need for symmetry breaking. The EP in a non-Hermitian system occurs when two or more eigenstates coalesce, which is usually associated with a non-Hermitian phase transition [12]. In a parity-time (\mathcal{PT})-symmetric non-Hermitian system (or other similar systems), the \mathcal{PT} symmetry of the eigenstates spontaneously breaks at the EP, which determines the exact \mathcal{PT} -symmetric phase and the broken \mathcal{PT} -symmetric phase in this system. The EP plays a pivotal role in intriguing dynamics and applications including asymmetric mode switching [23], unidirectional lasing [21,24,25], and enhanced optical sensing [26–33]. Recently, EP dynamics has been employed to engineer a target quantum state [34–37] and probe quantum phase transitions [38]. The mechanism of such a scheme is setting the target state as the coalescing state of a non-Hermitian Hamiltonian. In general, a familiar target state as the central resource of quantum information processing is always an eigenstate of a Hermitian system, such as a topological state, or a many-particle entangled state. It therefore requires the coalescing state to be Hermitian related and robust to the perturbation.

The aim of this paper is to provide a method for setting a target quantum state to be a coalescing state. As is well known, an EP is exclusive for non-Hermitian systems and is distinct from a degeneracy point (DP). We will show that the transition from a DP for a Hermitian system to an EP can be realized by proper non-Hermitian terms. This theorem indicates that, for a general Hermitian system with a DP, one of the degenerate eigenstates can be set as a coalescing state of a non-Hermitian system. This allows the scheme to prepare a target quantum state based on the EP dynamics. To illustrate the theorem, we investigate an exactly solvable quasi-one-dimensional model, which supports the transition between fully degenerate and exceptional spectra. It is shown that such a model in the thermodynamic limit is equivalent to a two-coupled ring with a power-law decay long-range hopping term. As its application, we also study the EP dynamics for generating coalescing edge modes in Su-Schrieffer-Heeger (SSH)-like models. This finding provides a way to construct a non-Hermitian system with an EP based on a Hermitian system with a DP. The advantage of this method is that the coalescing state is the eigenstate of a Hermitian system and is robust to the strength of the non-Hermitian term. We expect our results to benefit experimental research.

This paper is organized as follows. In Sec. II, we present a theorem for a general system to create robust EPs from DPs. In Secs. III and IV, we illustrate the theorem using two examples. In Sec. V, we propose a dynamic scheme to prepare edge modes as the application of the theorem. Finally, we provide a summary in Sec. VI.

II. THEOREM ON ROBUST EP FROM DP

A general system at an EP is obtained by tuning an imaginary parameter, such as an imaginary potential or flux, to switch real energy levels to complex ones. The critical value of the parameter is usually the solution of a transcendental

^{*}songtc@nankai.edu.cn

equation, and the EP system is sensitive to the imaginary parameter. Then it is a little difficult to set an EP system precisely in practice. The main aim of this paper is to answer the question of whether a robust EP system can be obtained. In this section, we present a theorem on establishing an EP based on a DP of a Hermitian system. The obtained EP is not sensitive to the strength of the non-Hermitian parameters.

We consider a general non-Hermitian Hamiltonian in the form

$$H = H_0 + H', \quad (1)$$

which can be separated into two parts, Hermitian and non-Hermitian ones, i.e.,

$$H_0 = (H_0)^\dagger, \quad \text{but } H' \neq (H')^\dagger. \quad (2)$$

Theorem. Hamiltonian $H = H_0 + H'$ must possess an EP in its spectrum if it is constructed under the following conditions:

(i) Hamiltonian H_0 has twofold degenerate eigenstates $|A\rangle$ and $|B\rangle$ with eigenvalue E .

(ii) $|A\rangle$ ($|B\rangle$) is a nondegenerate eigenvector of H (H^\dagger) with eigenvalue E .

Proof. Based on the assumptions on H (H^\dagger), two states $|A\rangle$ and $|B\rangle$, we have

$$H|A\rangle = E|A\rangle, \quad H^\dagger|B\rangle = E|B\rangle. \quad (3)$$

It means that two states $|A\rangle$ and $|B\rangle$ are mutually biorthogonally conjugate and the biorthogonal norm of them is $\langle B|A\rangle$. Condition (i) states $\langle B|A\rangle = 0$. According to the theory of non-Hermitian systems [2,39–41], the vanishing norm indicates that state $|A\rangle$ is a coalescing state of H , i.e., Hamiltonian H gets an EP.

So when a Hermitian Hamiltonian H_0 and a non-Hermitian Hamiltonian H (H^\dagger) have a common eigenstate $|A\rangle$ ($|B\rangle$) with a corresponding energy E , and in the meantime $|A\rangle$ is degenerate for H_0 but not degenerate for H , one can say that Hamiltonian H gets an EP. The theorem is given here without specific reference to the detailed form of the Hamiltonian. It should work for nonrelativistic and relativistic, continuous and discrete Hamiltonians. Applying it to a tight-binding model, we can find some detailed signatures of the degenerate eigenstates. One can get $H'|A\rangle = 0$ and $(H')^\dagger|B\rangle = 0$ according to the two conditions. The simplest example for such a H' is a unidirectional hopping term, i.e., $\kappa a_i^\dagger a_j$ ($i \neq j$), where a_i and a_j are fermion or boson operators. Note that the above conditions can be satisfied if $a_j|A\rangle = 0$ and $a_i|B\rangle = 0$. It means that the two states $|A\rangle$ and $|B\rangle$ have nodal points at j and i , respectively. In addition, the existence of an EP is independent of the nonzero value of κ . Notably, states $|A\rangle$ ($|B\rangle$) can be multifermion or boson states. Considering an n -boson system, we have

$$|A\rangle = \frac{1}{\sqrt{n!}}(a_i^\dagger)^n|\text{Vac}\rangle, \quad |B\rangle = \frac{1}{\sqrt{n!}}(a_j^\dagger)^n|\text{Vac}\rangle, \quad (4)$$

where $|\text{Vac}\rangle$ is the vacuum state, and we still have $H'|A\rangle = 0$ and $(H')^\dagger|B\rangle = 0$ from the fact that $a_j|A\rangle = 0$ and $a_i|B\rangle = 0$.

Then for the initial state

$$|\psi(0)\rangle = |B\rangle = \frac{1}{\sqrt{n!}}(a_j^\dagger)^n|\text{Vac}\rangle, \quad (5)$$

the evolved state is

$$\begin{aligned} |\psi(t)\rangle &= \exp(-iHt)|B\rangle \\ &= \frac{\exp(-inEt)}{\sqrt{n!}} \sum_{m=0}^n \frac{(-ikt a_i^\dagger a_j)^m}{m!} (a_j^\dagger)^n |\text{Vac}\rangle. \end{aligned} \quad (6)$$

For a long timescale, we have

$$|\psi(t)\rangle \propto (\kappa t)^n |A\rangle, \quad (7)$$

which indicates that the system has the behavior of an $(n+1)$ -order EP [28,42–44]. This rigorous conclusion has important implications in the design of quantum devices to prepare a target quantum state at will, which can be a topological insulating state [45] and quantum spin states [37]. In the following sections, we will present several illustrative examples to demonstrate the theorem.

III. ZERO POINT IN REAL SPACE

Consider a uniform $2N$ -site ring system with the Hamiltonian

$$H_0 = \sum_{j=1}^{2N} (a_j^\dagger a_{j+1} + \text{H.c.}) = 2 \sum_k \cos ka a_k^\dagger, \quad (8)$$

where

$$a_k^\dagger = \frac{1}{\sqrt{2N}} \sum_{j=1}^{2N} e^{ikj} a_j^\dagger, \quad (9)$$

with the wave vector $k = \pi n/N$, $n = 1, 2, \dots, 2N$. a_j^\dagger is the creation operator of the fermion or boson at the j th site. We note that there are $N-1$ pairs of degenerate eigenstates. The aim of this section is to answer the question of what kind of H' can result in the transition from a DP to EP. Here, we only focus on a single-particle case, and the extension for multiboson and fermion cases is straightforward. For H_0 , a single-particle eigenstate has the form

$$|k\rangle = \frac{1}{\sqrt{2N}} \sum_{j=1}^{2N} e^{ikj} |j\rangle, \quad (10)$$

which has no nodal point for any k . Here, $|j\rangle = a_j^\dagger|\text{Vac}\rangle$ is the position state. However, we can construct twofold degenerate eigenstates in the form

$$|\psi_k^\pm\rangle = \frac{1}{\sqrt{2}}(|k\rangle \pm e^{i2kl_0}|-k\rangle), \quad (11)$$

with $\langle \psi_k^+ | \psi_k^- \rangle = 0$. The additional factor e^{i2kl_0} leads to a nodal point at the l_0 th site, i.e.,

$$\langle l_0 | \psi_k^- \rangle = 0. \quad (12)$$

It is easy to check that for another state $|\psi_k^+\rangle$, there is a nodal point at the (l_0+r) th site, i.e.,

$$\langle l_0+r | \psi_k^+ \rangle = 0, \quad (13)$$

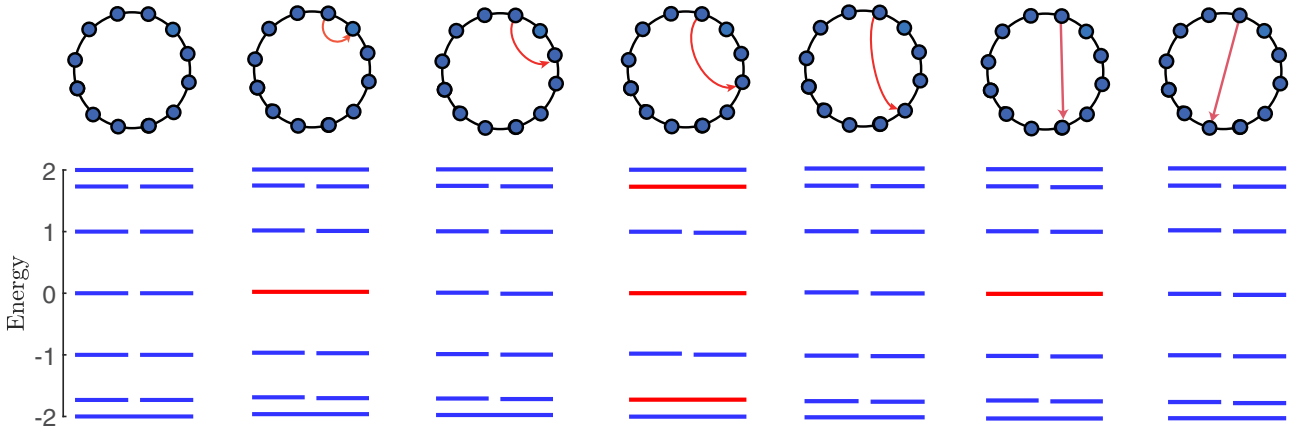


FIG. 1. Schematic illustration of the levels of a Hermitian 12-site ring, which shows the effect of an additional single unidirectional hopping (red arrow) crossing two sites. Two degenerate levels are indicated by a pair of blue segments, while a coalescing level is in red. The parameter for the red arrow is $\kappa = 0.5$. We can see that a single asymmetric hopping term for a Hermitian ring can drive the transition between a DP and EP for some specific but not all levels.

when the following condition is satisfied,

$$\cos(kr) = 0, \quad (14)$$

which requires k to have specific values

$$k = \frac{(2m+1)\pi}{2r}, \quad m = 0, 1, 2, \dots \quad (15)$$

Then the non-Hermitian term H' is in the form

$$H' = \kappa a_0^\dagger a_{l_0+r}. \quad (16)$$

For instance, for $r = 1$, we have $k = \pi/2$, and for $r = 2$, we have $k = \pi/4$ and $k = 3\pi/4$. It means that one can take $H' = \kappa a_0^\dagger a_{l_0+1}$ to acquire the coalescing state $|\psi_{\pi/2}^+\rangle$, while taking $H' = \kappa a_0^\dagger a_{l_0+2}$ to obtain $|\psi_{3\pi/4}^+\rangle$. In Fig. 1, we schematically illustrate a finite system with several kinds of non-Hermitian hopping terms and plot the corresponding energy levels. It indicates that for the finite system, there are some DPs that cannot be transmitted to EPs by a single asymmetric hopping term.

IV. ZERO POINT IN K SPACE

In the previous section, we have shown that a single asymmetric hopping term for a Hermitian ring can drive the transition between a DP and EP for some specific but not all levels. A natural question is what kind of H' can result in the transition from a DP to an EP for any given k . Actually, this can be done by simply taking $H'_k = J a_k^\dagger a_{-k}$, which contains all range unidirectional hopping terms. In the above example, $H' = \kappa a_i^\dagger a_j$, we do not restrict a_i^\dagger and a_j to be the operators in real space. For example, an EP Hamiltonian can be $H' = \kappa a_{k_1}^\dagger a_{k_2}$. The corresponding coalescing state is $a_{k_1}^\dagger |\text{Vac}\rangle_{k_1} |\text{Vac}\rangle_{k_2}$, while the auxiliary state is $a_{k_2}^\dagger |\text{Vac}\rangle_{k_1} |\text{Vac}\rangle_{k_2}$.

Now we investigate an example to demonstrate the application of the above result. We consider a system with the non-Hermitian term

$$H' = \sum_{\pi \geq k > 0} H'_k = \sum_{\pi > k > 0} a_k^\dagger a_{-k} + \frac{1}{2}(a_0^\dagger a_0 + a_\pi^\dagger a_\pi). \quad (17)$$

a_k^\dagger is the creation operator of the fermion or boson with momentum k in momentum space. In the case of $k \neq 0$ and π , both $H'_k |k\rangle = 0$ and $(H'_k)^\dagger |-k\rangle = 0$ always hold for arbitrary k , which indicates H' drives all DPs into EPs. A straightforward derivation leads to

$$H' = \frac{1}{2N} \sum_{l+j=\text{odd}(l>j)} i \cot\left[\frac{(l+j)\pi}{2N}\right] (a_l^\dagger a_j + \text{H.c.}) + \frac{1}{2} \sum_{l+j=2N, 4N} a_l^\dagger a_j, \quad (18)$$

where the system size in real space is $2N$, i.e., $l, j = 1 \dots 2N$. In Fig. 2(a), we schematically illustrate a finite system with the above H' . We note that the non-Hermitian hopping strength $i \cot[(l+j)\pi/(2N)]/(2N)$ is as large as $l+j$ close to 0, $2N$, and $4N$. For $l+j = 2N+1$, we have $l-j = 2N+1-2j$, which indicates long-range hopping. For example, taking $j = N/2$, we have $l = 3N/2+1$. Then the hopping spacing is $l-j = N+1$. However, if we reshape the ring as a ladder, such long-range hopping terms become short range as shown in Fig. 2(b). We can rewrite the distance between two sites, i.e., $l+j$, as $l+j = 2nN + \Delta$ ($\Delta = \pm 1, \pm 3, \dots$, and $n = 0, 1$), and considering the case with $\Delta \ll 2N$, we can simplify the coupling constant

$$\frac{1}{2N} \cot\left[\frac{(l+j)\pi}{2N}\right] = \frac{1}{\Delta\pi} + \frac{1}{2N} O\left(\frac{\Delta\pi}{2N}\right). \quad (19)$$

This example indicates that for the finite system, $2N-1$ pairs of degenerate levels can be switched into $2N-1$ coalescing levels by H' .

The underlying mechanism of realizing the transition from a degeneracy spectrum to a coalescing spectrum can be revealed by the following model. Inspired by Eq. (19), we consider a two-coupled uniform chain system, which has a two-leg ladder structure. Figure 2(c) sketches the geometry of the system, in which the hopping amplitudes in each leg are uniform and the hopping strengths are distance dependent. Such a ladder system is a bipartite lattice system, consisting of two sublattices A and B . We write down the Hamiltonian

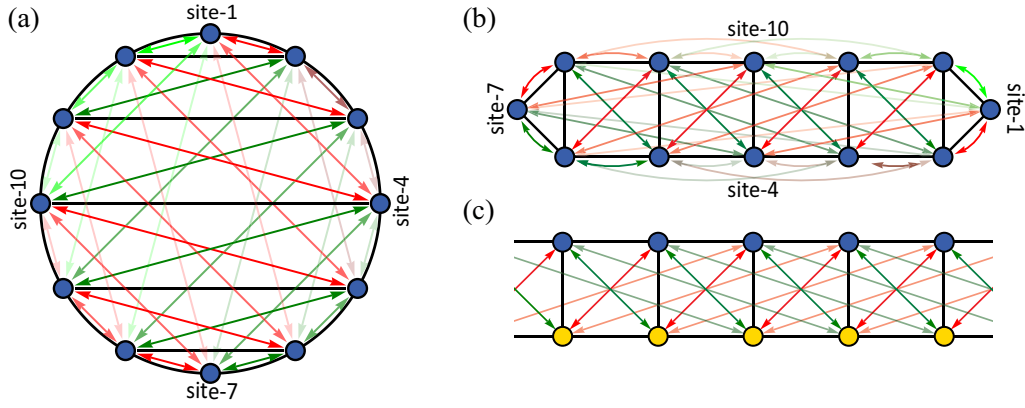


FIG. 2. (a) The schematic diagram of Hamiltonian in Eq. (18). The black straight lines denote the real long-range couplings. The colored lines with bidirectional arrows denote the pure imaginary couplings, and we adopt different colors and opacities to distinguish the imaginary couplings. The dark red lines represent the coupling where the sum of the site's position is equal to 5 or 3, and we further distinguish 5 and 3 by the reduced transparency. The same goes for the green lines standing for 23, 21, 19, the dark green lines for 11, 9, 7, and the red lines for 17, 15, 13. (b) We reshape the schematic diagram of (a) to be a ladder system. (c) A schematic illustration of the Hamiltonian in Eq. (20). The black ladder represents H_0 , and the colored lines with bidirectional arrows denote H' . Ignoring the hoppings on the boundary, the intralayer long-range hoppings for (b) and (c) have the same linking method but different strengths.

for the system in the form

$$H_0 = \sum_{j=1}^N (\alpha_j^\dagger \beta_j + \alpha_j^\dagger \alpha_{j+1} + \beta_j^\dagger \beta_{j+1} + \text{H.c.}), \quad (20)$$

$$H' = \frac{iJ}{2} \sum_{j=1}^N \sum_{n=1}^N \frac{1}{2n-1} (\alpha_j^\dagger \beta_{j+2n-1} - \beta_j^\dagger \alpha_{j+2n-1} + \text{H.c.}),$$

where α_l^\dagger and β_l^\dagger are the creation operators of the fermion or boson at the l th site of sublattice A and B , respectively. We take a periodic boundary condition by setting $\alpha_{N+1}^\dagger = \alpha_1^\dagger$ and $\beta_{N+1}^\dagger = \beta_1^\dagger$. Taking the transformation

$$\begin{aligned} \alpha_k &= \frac{1}{\sqrt{N}} \sum_j e^{ikj} \alpha_j, \\ \beta_k &= \frac{1}{\sqrt{N}} \sum_j e^{ikj} \beta_j, \end{aligned} \quad (21)$$

we have

$$H = \sum_k H_k = \sum_k (\alpha_k^\dagger, \beta_k^\dagger) h_k \begin{pmatrix} \alpha_k \\ \beta_k \end{pmatrix}, \quad (22)$$

where the wave vector $k = \pi(2n - N)/N$ ($n = 0, 1, \dots, N - 1$). The Bloch Hamiltonian is

$$h_k = \begin{pmatrix} 0 & 1 - \Delta_k \\ 1 + \Delta_k & 0 \end{pmatrix} + 2 \cos k, \quad (23)$$

where

$$\Delta_k = J \sum_{n=1}^N \frac{\sin[(2n-1)k]}{2n-1}. \quad (24)$$

The Hamiltonian H can be easily diagonalized since $[H_k, H_{k'}] = 0$, and the spectrum is

$$\varepsilon_k = 2 \cos k \pm \sqrt{1 - (\Delta_k)^2}. \quad (25)$$

We note that when the summation in Δ_k covers to infinity, Δ_k is a step function

$$\Delta_k = \frac{J\pi}{4} \text{sgn}(k), \quad (26)$$

according to Fourier analysis. Then the spectrum becomes

$$\varepsilon_k = \pm \sqrt{1 - (J\pi/4)^2}, \quad (27)$$

which vanishes at $J = 4/\pi$ and the EP spectrum appears.

V. EMERGING EDGE MODES

In the above sections, the obtained coalescing states are all extended states, which have real wave vectors. In this section, we focus on the transition from a DP to EP where the coalescing bound states appear. A coalescing bound state is a local state and lives at an energy gap, and then can be a stable target state of the time evolution at an EP. In the following, we at first present two examples of coalescing edge states in SSH-like models. Then we study the dynamical preparation of a two-dimensional (2D) edge state.

A. SSH chain

We start our investigation by considering a SSH chain with single unidirectional hopping across two ends, with the Hamiltonian in the form

$$\begin{aligned} H_0 &= \frac{1}{2} \sum_{l=1}^{2N-1} [1 + (-1)^l \delta] a_l^\dagger a_{l+1} + \text{H.c.}, \\ H' &= \kappa a_1^\dagger a_{2N}, \end{aligned} \quad (28)$$

where a_l^\dagger is the creation operator of the fermion or boson at the l th site. It is a bipartite lattice, i.e., it has two sublattices A, B such that each site on lattice A has its nearest neighbors on sublattice B , and vice versa. The Hermitian system H_0 is the prototype of a topologically nontrivial band insulator with a symmetry-protected topological phase [46,47]. In recent years, it has attracted much attention and extensive studies have been demonstrated [48–53]. The degenerate zero modes take the role of a topological invariant in the infinite N limit

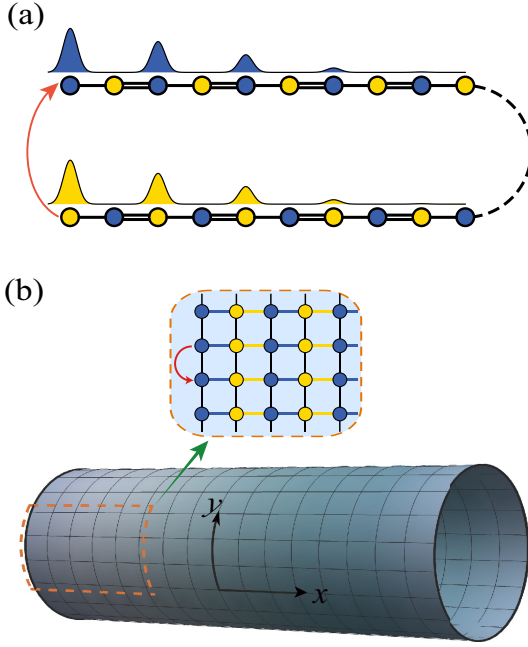


FIG. 3. (a) Schematic illustration of the SSH chain. The unidirectional hopping κ pointing from the head to the tail of the SSH chain is denoted by a red arrow. Two degenerate edge states $|R\rangle$ (yellow) and $|L\rangle$ (blue) appear when taking $\kappa = 0$. When $\kappa \neq 0$, there only exists a coalescing state $|L\rangle$. (b) Schematic illustration of the SSH cylinder. The details of the couplings are shown in the inset, wherein the unidirectional coupling is indicated by the red arrow.

and are explicitly expressed as

$$\begin{aligned} |L\rangle &= \frac{1}{\sqrt{\Omega}} \sum_{j=1}^N \left(\frac{\delta-1}{\delta+1}\right)^{j-1} a_{2j-1}^\dagger |\text{Vac}\rangle, \\ |R\rangle &= \frac{1}{\sqrt{\Omega}} \sum_{j=1}^N \left(\frac{\delta-1}{\delta+1}\right)^{N-j} a_{2j}^\dagger |\text{Vac}\rangle, \end{aligned} \quad (29)$$

for $\delta > 0$ where the normalization factor is $\Omega = \{1 - [(\delta-1)/(\delta+1)]^{2N}\} / \{1 - [(\delta-1)/(\delta+1)]^2\}$. It is easy to check that

$$a_{2N}|L\rangle = a_1|R\rangle = 0, \quad (30)$$

which results in

$$H'|L\rangle = (H')^\dagger|R\rangle = 0. \quad (31)$$

According to the aforementioned theorem, $|L\rangle$ is a coalescing edge state. In previous work [54], it has been shown that two bound states appear in the bulk of a chain when a strong bond is replaced by a tiny one. Now we take it as a unidirectional hopping as described in H' . In this sense, it is not surprising that a single bound state $|L\rangle$ can appear in the bulk of a finite size but sufficiently long chain. The profiles of the edge modes are schematically illustrated in Fig. 3(a). In contrast, when the unidirectional hopping replaces a weak bond, no zero mode appears. Therefore, the topological feature can be demonstrated by adding a non-Hermitian impurity, as a generalization of the bulk-edge correspondence.

B. SSH cylinder

A similar situation can occur in a 2D system by adding a local non-Hermitian impurity. In the following we present an example of a 2D system, which is an extended 2D SSH cylinder. The 2D SSH cylinder consists of M (even) chains which are uniformly coupled,

$$\begin{aligned} H_{\text{sc}}^0 &= \sum_{j=1}^M \sum_{l=1}^{2N-1} [1 + (-1)^l \delta] a_{j,l}^\dagger a_{j,l+1} \\ &+ J \sum_{j=1}^M \sum_{l=1}^{2N} a_{j,l}^\dagger a_{j+1,l} + \text{H.c.}, \end{aligned} \quad (32)$$

and a perturbation on the boundary,

$$H'_{\text{sc}} = \kappa a_{1,1}^\dagger a_{M,1}, \quad (33)$$

where j (l) is the index of row (column), and $a_{j,l}^\dagger$ is the creation operator of the fermion or boson at the site (j, l) . Therefore, the Hamiltonian of the SSH cylinder reads $H_{\text{sc}} = H_{\text{sc}}^0 + H'_{\text{sc}}$. Figure 3(b) shows the schematic illustration of the SSH cylinder, where the red arrow in the inset represents the perturbation. H_{sc}^0 has four degenerate local zero modes, two of which localize at the left boundary,

$$\begin{aligned} |L_e\rangle &= \frac{1}{\sqrt{\Omega}} \sum_{j=1}^{M/2} \sum_{l=1}^N \left(\frac{\delta-1}{\delta+1}\right)^{l-1} a_{2j,2l-1}^\dagger |\text{Vac}\rangle, \\ |L_o\rangle &= \frac{1}{\sqrt{\Omega}} \sum_{j=1}^{M/2} \sum_{l=1}^N \left(\frac{\delta-1}{\delta+1}\right)^{l-1} a_{2j-1,2l-1}^\dagger |\text{Vac}\rangle, \end{aligned} \quad (34)$$

where $\Omega = M/2\{1 - [(\delta-1)/(\delta+1)]^N\} / \{1 - [(\delta-1)/(\delta+1)]^2\}$. It is not hard to check that

$$H'_{\text{sc}}|L_o\rangle = 0, \quad (H'_{\text{sc}})^\dagger|L_e\rangle = 0, \quad (35)$$

which means $|L_o\rangle$ is a coalescing edge state of H_{sc} , and $|R_{e(o)}\rangle$ remain degenerate states, $H|R_{e(o)}\rangle = 0$.

C. Dynamical preparation of edge state

It seems that DP and EP systems are totally different. Taking $H' \rightarrow \kappa H'$ to impose a strength on the non-Hermitian term, one can investigate the effect of H' on the system quantitatively. Intuitively, a small change of κ from zero can result in a drastic change. However, in the following, we will show that there exists a continuous crossover between them. We measure the signature of the system by detecting the dynamics of the observable, such as the time evolution of particle probability. As the application of the theorem, the relationship between time and particle probability is another approach to prepare the edge modes.

We consider a two-site system as the simplest example for the obtained theorem, which has the Hamiltonian

$$H_{2s} = \kappa a_1^\dagger a_2 + \varepsilon_0 (a_1^\dagger a_1 + a_2^\dagger a_2), \quad (36)$$

where a_i^\dagger ($i = 1, 2$) is the creation operator of the fermion or boson. The time evolution operator has the form

$$\begin{aligned} U(t) &= \exp(-iH_{2s}t) \\ &= \exp[-i\varepsilon_0(a_1^\dagger a_1 + a_2^\dagger a_2)t] \exp(-i\kappa a_1^\dagger a_2 t), \end{aligned} \quad (37)$$

which drives the time evolution for an initial state $|\psi(0)\rangle$,

$$|\psi(t)\rangle = U(t)|\psi(0)\rangle. \quad (38)$$

(i) In the case of $\kappa = 0$, we have

$$|\psi(t)\rangle = \exp[-i\varepsilon_0(a_1^\dagger a_1 + a_2^\dagger a_2)t]|\psi(0)\rangle. \quad (39)$$

Then for an initial state with fixed particle number, i.e., $(a_1^\dagger a_1 + a_2^\dagger a_2)|\psi(0)\rangle = n|\psi(0)\rangle$ with n being the particle number, $U(t)$ only contributes a phase factor to $|\psi(0)\rangle$.

(ii) In the case of $\kappa \neq 0$, we have

$$\exp(-i\kappa a_1^\dagger a_2 t) = \sum_{m=0}^{\infty} \frac{1}{m!} (-i\kappa a_1^\dagger a_2 t)^m. \quad (40)$$

Then the time evolution of the coalescing state $|\psi_c\rangle = a_1^\dagger|\text{Vac}\rangle$ is

$$U(t)|\psi_c\rangle = \exp(-i\varepsilon_0 t)|\psi_c\rangle, \quad (41)$$

while the time evolution of the auxiliary state $|\psi_a\rangle = a_2^\dagger|\text{Vac}\rangle$ is

$$U(t)|\psi_a\rangle = \exp(-i\varepsilon_0 t)(|\psi_a\rangle - i\kappa t|\psi_c\rangle), \quad (42)$$

where we have used the identity $(a_1^\dagger a_2)^2|\psi_a\rangle = 0$. The difference between a DP and EP is obvious when $\kappa t \gg 1$. However, within the timescale $t \ll 1/\kappa$, the dynamics under the DP and EP has no difference. It indicates that the crossover from a DP to EP is continuous. Similarly, it has been shown that a non-Hermitian system around an EP exhibits some peculiar critical dynamics as an EP [36]. For a multiboson case, see Eq. (6).

Equation (42) indicates that the time evolution of the coalescing state linearly depends on time t , so the evolved state is approximately equal to $|\psi_c\rangle$ for the relatively large timescale. When $|\psi_c\rangle$ is a localized coalescing state, the dynamical preparation of the robust edge state is as follows. Consider the time evolution driven by Hamiltonian H_{sc} , so the initial state is

$$|\psi(0)\rangle = \frac{1}{\sqrt{M/2}} \sum_{j=1}^{M/2} a_{2j-1,1}^\dagger |\text{Vac}\rangle, \quad (43)$$

which is just $|L_c\rangle$ when δ infinitely approaches 1. Figure 4(a) exhibits numerical simulations of $|\psi(t)\rangle$, where the system size is $N = 100$, $M = 20$. We only show the region $N \leq 30$ because the probability is almost zero in the other region. Figure 4(b) exhibits the fidelity

$$F(t) = \langle L_o | \psi(t) \rangle \quad (44)$$

to evaluate the closeness of the evolved state $|\psi(t)\rangle$ and the coalescing edge state $|L_o\rangle$. In Fig. 4(a), we show the probability distribution of $|\psi(0)\rangle$ in the real space, where the fidelity is almost zero. Before $t = 100$, the probability distribution of $|\psi(t)\rangle$ is presented as an unstable stripe, and the fidelity has a small value. At $t = 200$, the stripe tends to be stable and is similar in appearance to the edge state, where the fidelity reaches to around 0.9. At $t = 800$, we get a stable stripe, and the fidelity is close to 1 which indicates that $|\psi(t)\rangle$ is the coalescing edge state. Our numerical results show that the EP dynamics based scheme has better efficiency. The setting of the system parameters is expected to provide guidance for the experiment.

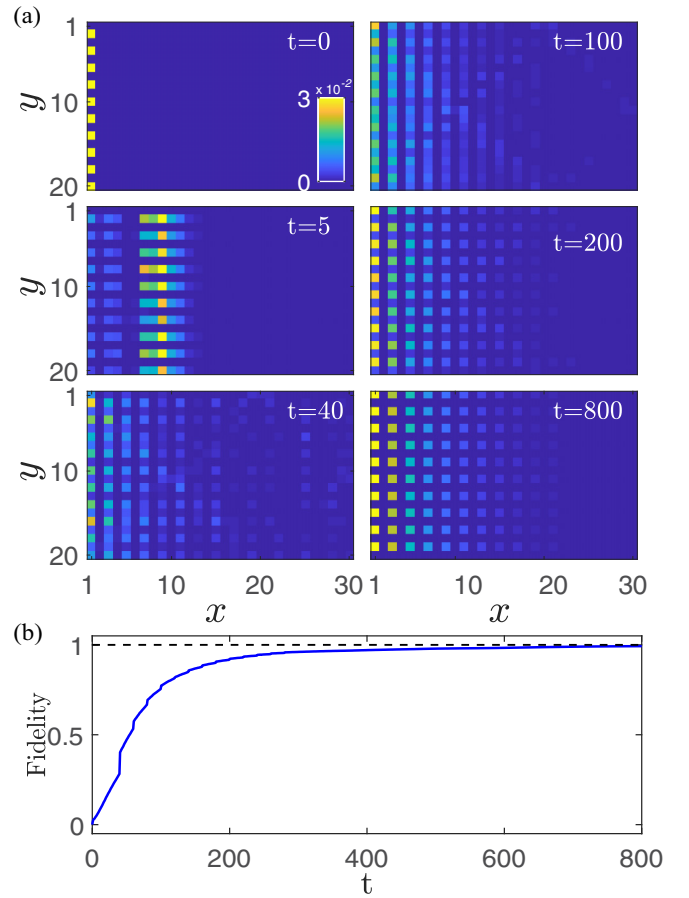


FIG. 4. (a) Snapshots of the probability distribution at various time moments for initial excitation in Eq. (43). The probability is normalized at any moment. The system size is $M = 20$, $N = 100$. Only the limited region within $N = 30$ is shown because the intensity is almost vanishing outside this area. The other parameters are $\delta = 0.1$, $J = 1$, and $\kappa = 0.5$. (b) The fidelity between the evolved state $|\psi(t)\rangle$ and the coalescing edge state $|L_o\rangle$. The units of time are $1/J$.

VI. SUMMARY

In summary, we have developed a theory for a class of non-Hermitian Hamiltonians which supports robust EPs. Such a Hamiltonian consists of two separate parts, the Hermitian and non-Hermitian ones. The Hermitian Hamiltonian has degenerate eigenstates, which coalesce into a single state by the non-Hermitian part. The most fascinating and important feature of such systems is that the EP is not sensitive to the strength of the non-Hermitian perturbation. As examples, we have investigated three types of systems: (i) a uniform ring system with a single asymmetric hopping term, in which several pairs of degenerate states become coalescing states, (ii) a uniform ladder system with long-range power-law decaying imaginary hopping terms, in which the degenerate spectrum becomes a coalescing spectrum, and (iii) a SSH-like system in a nontrivial topological phase with a single asymmetric hopping term, in which the degenerate edge state becomes a coalescing edge state. We also demonstrated the application of the EP dynamics based on a numerical simulation. It was shown that the 2D coalescing edge state can be generated by a local initial state. Our findings offer a

method for the efficient construction of a robust EP system and are expected to be necessary and insightful for quantum engineering.

ACKNOWLEDGMENTS

This work was supported by National Natural Science Foundation of China (under Grant No. 11874225).

-
- [1] C. M. Bender, Making Sense of non-Hermitian Hamiltonians, *Rep. Prog. Phys.* **70**, 947 (2007).
- [2] N. Moiseyev, *Non-Hermitian Quantum Mechanics* (Cambridge University Press, Cambridge, U.K., 2011).
- [3] A. Krasnok, D. Baranov, H. Li, M. A. Miri, F. Monticone, and A. Alú, Anomalies in light scattering, *Adv. Opt. Photonics* **11**, 892 (2019).
- [4] A. Guo, G. J. Salamo, D. Duchesne, R. Morandotti, M. Volatier-Ravat, V. Aimez, G. A. Siviloglou, and D. N. Christodoulides, Observation of \mathcal{PT} -Symmetry Breaking in Complex Optical Potentials, *Phys. Rev. Lett.* **103**, 093902 (2009).
- [5] C. E. Rüter, K. G. Makris, R. El-Ganainy, D. N. Christodoulides, M. Segev, and D. Kip, Observation of parity-time symmetry in optics, *Nat. Phys.* **6**, 192 (2010).
- [6] B. Peng, S. K. Özdemir, F. Lei, F. Monifi, M. Gianfreda, G. L. Long, S. Fan, F. Nori, C. M. Bender, and L. Yang, Parity-time-symmetric whispering-gallery microcavities, *Nat. Phys.* **10**, 394 (2014).
- [7] L. Feng, Z. J. Wong, R. M. Ma, Y. Wang, and X. Zhang, Single-mode laser by parity-time symmetry breaking, *Science* **346**, 972 (2014).
- [8] H. Hodaei, M. A. Miri, M. Heinrich, D. N. Christodoulides, and M. Khajavikhan, Parity-time-symmetric microring lasers, *Science* **346**, 975 (2014).
- [9] L. Feng, R. El-Ganainy, and L. Ge, Non-Hermitian photonics based on parity-time symmetry, *Nat. Photonics* **11**, 752 (2017).
- [10] S. Longhi, Parity-time symmetry meets photonics: A new twist in non-Hermitian optics, *Eur. Phys. Lett.* **120**, 64001 (2017).
- [11] R. El-Ganainy, K. G. Makris, M. Khajavikhan, Z. H. Musslimani, S. Rotter, and D. N. Christodoulides, Non-Hermitian physics and \mathcal{PT} -symmetry, *Nat. Phys.* **14**, 11 (2018).
- [12] M. A. Miri and A. Alú, Exceptional points in optics and photonics, *Science* **363**, eaar7709 (2019).
- [13] S. K. Özdemir, S. Rotter, F. Nori, and L. Yang, Parity-time symmetry and exceptional points in photonics, *Nat. Mater.* **18**, 783 (2019).
- [14] Y. Wu, W. Q. Liu, J. P. Geng, X. R. Song, X. Y. Ye, C. K. Duan, X. Rong, and J. F. Du, Observation of parity-time symmetry breaking in a single-spin system, *Science* **364**, 878 (2019).
- [15] L. Jin and Z. Song, Scaling behavior and phase diagram of a \mathcal{PT} -symmetric non-Hermitian Bose-Hubbard system, *Ann. Phys.* **330**, 142 (2013).
- [16] L. Jin and Z. Song, Hermitian dynamics in a class of pseudo-Hermitian networks, *Phys. Rev. A* **84**, 042116 (2011).
- [17] X. Z. Zhang and Z. Song, Momentum-independent reflectionless transmission in the non-Hermitian time-reversal symmetric system, *Ann. Phys.* **339**, 109 (2013).
- [18] A. Mostafazadeh, Spectral Singularities of Complex Scattering Potentials and Infinite Reflection and Transmission Coefficients at Real Energies, *Phys. Rev. Lett.* **102**, 220402 (2009).
- [19] S. Longhi and L. Feng, Unidirectional lasing in semiconductor microring lasers at an exceptional point, *Photonics Res.* **5**, B1 (2017).
- [20] X. Q. Li, X. Z. Zhang, G. Zhang, and Z. Song, Asymmetric transmission through a flux-controlled non-Hermitian scattering center, *Phys. Rev. A* **91**, 032101 (2015).
- [21] L. Jin and Z. Song, Incident Direction Independent Wave Propagation and Unidirectional Lasing, *Phys. Rev. Lett.* **121**, 073901 (2018).
- [22] L. Jin and Z. Song, Symmetry-protected scattering in non-Hermitian linear systems, *Chin. Phys. Lett.* **38**, 024202 (2021).
- [23] J. Doppler, A. A. Mailybaev, J. Böhm, U. Kuhl, A. Girschik, F. Libisch, T. J. Milburn, P. Rabl, N. Moiseyev, and S. Rotter, Dynamically encircling an exceptional point for asymmetric mode switching, *Nature (London)* **537**, 76 (2016).
- [24] H. Ramezani, S. Kalish, I. Vitebskiy, and T. Kottos, Unidirectional Lasing Emerging from Frozen Light in Nonreciprocal Cavities, *Phys. Rev. Lett.* **112**, 043904 (2014).
- [25] B. Peng, Ş. K. Özdemir, M. Liertzer, W. Chen, J. Kramer, H. Yılmaz, J. Wiersig, S. Rotter, and L. Yang, Chiral modes and directional lasing at exceptional points, *Proc. Natl. Acad. Sci. USA* **113**, 6845 (2016).
- [26] J. Wiersig, Enhancing the Sensitivity of Frequency and Energy Splitting Detection by Using Exceptional Points: Application to Microcavity Sensors for Single-Particle Detection, *Phys. Rev. Lett.* **112**, 203901 (2014).
- [27] Z. P. Liu, J. Zhang, Ş. K. Özdemir, B. Peng, H. Jing, X. Y. Lü, C. W. Li, L. Yang, F. Nori, and Y. X. Liu, Metrology with \mathcal{PT} -Symmetric Cavities: Enhanced Sensitivity Near the \mathcal{PT} -Phase Transition, *Phys. Rev. Lett.* **117**, 110802 (2016).
- [28] H. Hodaei, A. U. Hassan, S. Wittek, H. Garcia-Gracia, R. El-Ganainy, D. N. Christodoulides, and M. Khajavikhan, Enhanced sensitivity at higher-order exceptional points, *Nature (London)* **548**, 187 (2017).
- [29] W. Chen, S. K. Özdemir, G. Zhao, J. Wiersig, and L. Yang, Exceptional points enhance sensing in an optical microcavity, *Nature (London)* **548**, 192 (2017).
- [30] H. K. Lau and A. A. Clerk, Fundamental limits and non-reciprocal approaches in non-Hermitian quantum sensing, *Nat. Commun.* **9**, 4320 (2018).
- [31] M. Zhang, W. Sweeney, C. W. Hsu, L. Yang, A. D. Stone, and L. Jiang, Quantum Noise Theory of Exceptional Point Amplifying Sensors, *Phys. Rev. Lett.* **123**, 180501 (2019).
- [32] Y. H. Lai, Y. K. Lu, M. G. Suh, Z. Yuan, and K. Vahala, Observation of the exceptional-point-enhanced Sagnac effect, *Nature (London)* **576**, 65 (2019).
- [33] M. P. Hokmabadi, A. Schumer, D. N. Christodoulides, and M. Khajavikhan, Non-Hermitian ring laser gyroscopes with enhanced Sagnac sensitivity, *Nature (London)* **576**, 70 (2019).
- [34] T. E. Lee, F. Reiter, and N. Moiseyev, Entanglement and Spin Squeezing in Non-Hermitian Phase Transitions, *Phys. Rev. Lett.* **113**, 250401 (2014).
- [35] C. Li and Z. Song, Generation of Bell, W , and Greenberger-Horne-Zeilinger states via exceptional points in non-Hermitian quantum spin systems, *Phys. Rev. A* **91**, 062104 (2015).

- [36] X. M. Yang and Z. Song, Resonant generation of a p -wave Cooper pair in a non-Hermitian Kitaev chain at the exceptional point, *Phys. Rev. A* **102**, 022219 (2020).
- [37] X. Z. Zhang and Z. Song, Dynamical preparation of a steady ODLRO state in the Hubbard model with local non-Hermitian impurity, *Phys. Rev. B* **102**, 174303 (2020).
- [38] K. L. Zhang and Z. Song, Ising chain with topological degeneracy induced by dissipation, *Phys. Rev. B* **101**, 245152 (2020); Quantum Phase Transition in a Quantum Ising Chain at Nonzero Temperatures, *Phys. Rev. Lett.* **126**, 116401 (2021).
- [39] A. Mostafazadeh, Spectral singularities, biorthonormal systems and a two-parameter family of complex point interactions, *J. Phys. A: Math. Theor.* **42**, 125303 (2009).
- [40] N. Moiseyev, Critical phenomena associated with self-orthogonality in non-Hermitian quantum mechanics, *Europhys. Lett.* **62**, 789 (2003).
- [41] T. Kato, *Perturbation Theory of Linear Operators* (Springer, Berlin, 1966)
- [42] I. Mandal and E. J. Bergholtz, Symmetry and Higher-Order Exceptional Points, *Phys. Rev. Lett.* **127**, 186601 (2021).
- [43] W. D. Heiss, The physics of exceptional points, *J. Phys. A: Math. Theor.* **45**, 444016 (2012).
- [44] E. J. Bergholtz, J. C. Budich, and F. K. Kunst, Exceptional topology of non-Hermitian systems, *Rev. Mod. Phys.* **93**, 015005 (2021).
- [45] X. M. Yang and Z. Song, Quantum mold casting for topological insulating and edge states, *Phys. Rev. B* **103**, 094307 (2021).
- [46] S. Ryu and Y. Hatsugai, Topological Origin of Zero-Energy Edge States in Particle-Hole Symmetric Systems, *Phys. Rev. Lett.* **89**, 077002 (2002).
- [47] X. G. Wen, Symmetry-protected topological phases in non-interacting fermion systems, *Phys. Rev. B* **85**, 085103 (2012).
- [48] D. Xiao, M. C. Chang, and Q. Niu, Berry phase effects on electronic properties, *Rev. Mod. Phys.* **82**, 1959 (2010).
- [49] M. Z. Hasan and C. L. Kane, Colloquium: Topological Insulators, *Rev. Mod. Phys.* **82**, 3045 (2010); X. L. Qi and S. C. Zhang, Topological insulators and superconductors, *ibid.* **83**, 1057 (2011).
- [50] P. Delplace, D. Ullmo, and G. Montambaux, Zak phase and the existence of edge states in graphene, *Phys. Rev. B* **84**, 195452 (2011).
- [51] L. H. Li, Z. H. Xu, and S. Chen, Topological phases of generalized Su-Schrieffer-Heeger models, *Phys. Rev. B* **89**, 085111 (2014).
- [52] L. H. Li and S. Chen, Characterization of topological phase transitions via topological properties of transition points, *Phys. Rev. B* **92**, 085118 (2015).
- [53] S. Lin and Z. Song, Wide-range-tunable Dirac-cone band structure in a chiral-time-symmetric non-Hermitian system, *Phys. Rev. A* **96**, 052121 (2017).
- [54] C. Li, G. Zhang, S. Lin, and Z. Song, Quantum phase transition induced by real-space topology, *Sci. Rep.* **6**, 39416 (2016).